

# Experimental and Numerical Analysis of Delamination Repair Plaster Applied to Historical Masonry Building

Pietro Bocca, Silvio Valente, Alessandro Grazzini and Andrea Alberto

*Department of Structural, Building and Geotechnical Engineering, Politecnico di Torino, Torino 10129, Italy*

**Abstract:** Often masonry walls of historical buildings are subject to rising damp effects due to capillary or rain infiltrations. In the time, their cyclic action produces decay and delamination of historical plasters. An experimental laboratory procedure for the pre-qualification of repair mortars is described. Long-term plaster delamination frequently occurs because of the mechanical incompatibility of new repair mortars. The tested mortars are suitable for new dehumidified plasters applied to historical masonry walls. Compression static tests were carried out on composite specimens of stone block-repair mortar, which specific geometry can test the de-bonding process of mortar in adherence with historical masonry structure. A numerical simulation based on the cohesive crack model was used to follow the experimental data, in order to describe the evolutionary phenomenon of de-bonding as a function of a small number of parameters. This method supplies useful indication for selecting the product that is best in keeping with the mechanical characteristics of the historical material, thereby avoiding errors associated with materials that are not mechanically compatible. Currently, the methodology is being used at Sacro Monte di Varallo Special Natural Reserve (UNESCO heritage site) in Piedmont (Italy).

**Key words:** Historical masonry, dehumidified mortar, long-term plaster delamination, cohesive crack model.

## 1. Introduction

The restoration market offers a great number of dehumidified repair mortars to use as new transpiring plasters. Nevertheless, their mechanical and thermo-hygrometric characteristics have not been compared carefully with those of the historical masonry supports, often producing the failure of restoration work. Preventing this phenomenon is the main way of increasing the durability of repair work. The use of similar materials to historical ones in terms of mechanical, chemical and thermo-hygrometric performances is preferable [1, 2].

The goal of this experimental and numerical analysis, developed at the Non Destructive Testing Laboratory of the Politecnico di Torino, was to focus attention on the preliminary pre-qualification of repair materials before their use. The study of the

de-bonding process and the fatigue behavior of repair materials can avoid any mechanical or physical incompatibility, and at the same time to guarantee the maximum durability of restoration work [3, 4].

The methodology is being used at Sacro Monte di Varallo Special Natural Reserve (UNESCO heritage site). Situated at the top of the hill above the town of Varallo in Piedmont (Italy), Sacro Monte is an artistic-religious complex consisting of 45 chapels, which contain with frescoes and sculptures that tell the story of the life of Christ (Figs. 1 and 2). The aim of this particular architectural site was to reproduce the holy sites in Palestine where Christ had spent his early life. Constructed between the 15th and 18th centuries by the most important artists in Piedmont and Lombardy of that period, Sacro Monte is also a wonderful example of park gardens.

The chapels were constructed very simply, sometimes making use of natural materials, stone or brick walls, with wooden roofs and stone surfaces.

---

**Corresponding author:** Alessandro Grazzini, Ph.D., research fields: fatigue tests on strengthening materials, durability of restoration work, historical masonry seismic vulnerability and retrofit. E-mail: [alessandro.grazzini@polito.it](mailto:alessandro.grazzini@polito.it).



Fig. 1 Chapel n. 4—Joseph's dream.



Fig. 2 Chapel n. 28—Court of Herod.

Because of the rising capillary damp, the freeze-thaw cycles and the abundant rain and snow precipitations that characterize this mountain area, the historical plaster of the chapels has been subjected to progressive material decay over a long period of time (Figs. 3 and 4).

Since 2010, a research group of the Laboratory of non Destructive Testing Materials at the Politecnico di Torino has carried out particular tests on mixed stone block-mortar specimens in order to evaluate the



Fig. 3 Delamination and detachment of artistic plasters because of the rising damp effects due to capillary action or rain infiltration (Chapel n. 23—Jesus is taken).



Fig. 4 Decay of historical plasters because of the rain infiltrations (Chapel n. 13—The Temptations).

mechanical adhesion of the new repair mortars to the masonry supports. The aim of the research, called RE-FRESCOS project, was to offer appropriate technical solutions to stop this decay. In this way, it is possible to restore the masonry surfaces using compatible materials and techniques in order to save the frescos in the chapels.

The experimental results have been compared with a numerical analysis through the cohesive crack model. The parameters used in the numerical simulation of experimental tests were able to characterize the mechanical behaviour of the interface, in order to study the evolutionary phenomenon of plaster delamination. It is therefore possible to predict delamination in problems with different boundary conditions. The experimental and numerical results illustrated about the static tests represent the first step of this experimental study which is currently in progress. The

next steps will concern the same type of mixed specimens subjected to cyclic tests.

## 2. Materials and Experimental Setup

### 2.1 Single Mortar Specimens

The first stage of laboratory tests was the selection of a most compatible dehumidified repair mortar among two important products on the market. The tested repair mortars were labelled A and B. Both repaired products A and B were transparent pre-blended mortars made from NHL (natural hydraulic lime) and Eco-Pozzolan. This repair mortars were suitable for the restoration of historical masonry damaged by rising capillary damp and sulphate salts.

The mechanical and hygrometric characteristics of single materials have been investigated by means of 10 test pieces 40 mm × 40 mm × 160 mm for each mortar typology. All tests were carried out 28 days after the casting of repair mortar. The single specimens were labelled “M.A.” for mortar A and “M.B.” for mortar B, following the number code (Fig. 5).

Static tests, according to UNI EN 1015-11 and UNI 6556, were performed by means of a 250 kN model 810 M.T.S. (material testing system). In particular 3 specimens for each repair mortar were employed for bending test and 4 specimens for compressive and elastic modulus test.

Moreover on 3 specimens for each repair mortar were employed to carry out hygrometric test to determine the coefficient absorption of water for capillarity. The specimens, previously dried in oven to get a constant mass according to UNI EN 1015-18, were inserted vertically in a basin filled with water for a height of 10 mm. In this way, a face of specimen was absorbed (Fig. 6). The test was a duration of 24 hours, at the end the specimens were weighed to determine the value of damp mass which, together with the dry value, allowed to obtain the coefficient of absorption water for capillary.

### 2.2 Mixed Stone-Mortar Specimens

From the results of point 2.1, a typology of mortar was chosen and the experimental study was carried on with tests on composite stone block-repair mortar specimens. Compressive static tests were carried out on 4 specimens after 28 days of maturation. This mixed specimens were made by 30 mm thick layer of chosen repair mortar joining to the two shorter vertical sides of the stone block, selected similar to that of the Sacro Monti masonries (Fig. 7). The stone surfaces to contact with the mortar were treated by a specific pneumatic drill in order to improve the adherence of the strengthening product (Fig. 8).



Fig. 5 Compression test on single mortar specimen.

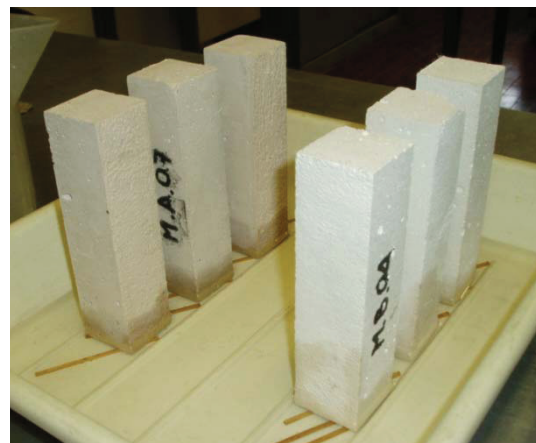


Fig. 6 Evaluation of the absorption coefficient of water for capillarity.

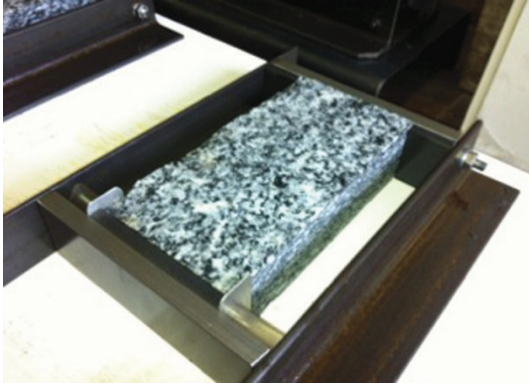


Fig. 7 Preparation of mixed specimen into steel mould.



Fig. 8 Adherence surface of stone treated by pneumatic drill.

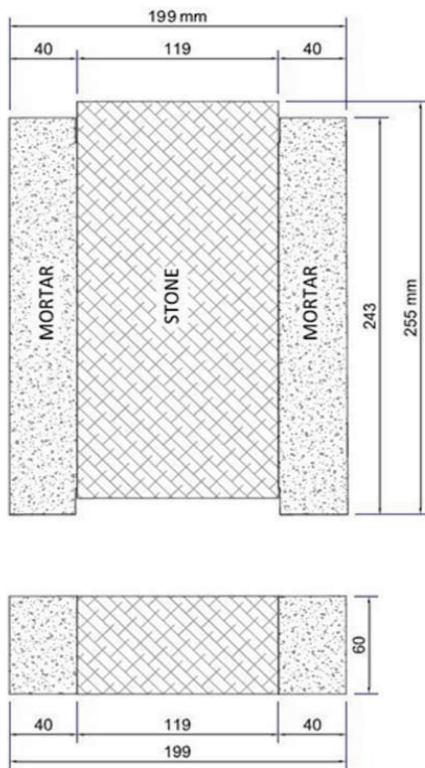


Fig. 9 Geometry of mixed specimen stone-repair mortar.

The ad hoc geometry of the stone block-mortar specimens (Fig. 9) was able to test the adherence between the repair mortar and the masonry structures.

The dehumidifying mortar layers were not applied in complete adherence with the stone block support, on the contrary, they were applied in symmetrical and regular discontinuity at the bottom and the top of the specimen (Fig. 9). These discontinuities behaved like notches that which were able to trigger multiple crack propagation, in order to simulate the adherence capacity of each repair mortar applied to a specific masonry wall as dehumidified plaster.

The mixed pieces were instrumented with two symmetrical couples of inductive displacement transducers (Fig. 10). One transducer per side was arranged horizontally in the lower part of the specimen and connected between the two opposite mortar layers, measuring the displacements due to bulging. The other transducers, one per side, were placed vertically on the stone block.

Monotonous compression tests were carried out by the controlling the horizontal opening with a speed opening at 0.0001 mm/s.

The lower mortars layer support was made up of a double system of steel wedges (Fig. 11), coupled with Teflon having thickness equal to 1 mm. It was for



Fig. 10 Composite specimen stone-repair mortar.

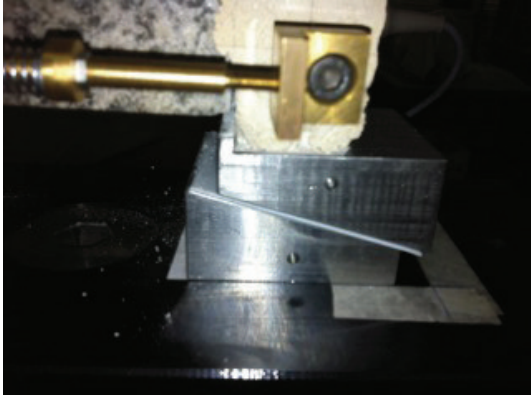


Fig. 11 Geometry of the wedges.

reducing the friction related to the horizontal expansion of the plaster, and so to stabilize the load curves.

The mixed specimens were labeled with SM (stone block-mortar), followed by a number indicating the order.

### 3. Experimental Results

#### 3.1 Single Repair Mortars

Table 1 shows the average values of mechanical (compressive stress  $\sigma$ , elastic modulus  $E$ ) and hygrometric characteristics (coefficient of absorption water for capillary  $W_{24}$ ) for the single specimens.

After the absorption capillary test, mortar B

displayed (Fig. 12) a great lift height capillary for mortar B (up to 80 mm), while for mortar A the absorption was limited to 50-60 mm (Fig. 13).

If regarding the mechanical characteristics, both repair mortars have displayed similar and comparable values with those of historical masonries. Instead about capillary absorption the repair products have showed a very different behavior. Mortar A displayed a great ability of water absorption and therefore it can give a improvement to damp masonry. Besides the lift height of water capillary in mortar A was smaller than mortar B, therefore for a long time this hygrometric characteristic will can do a shorter decay of repair mortar located in the inferior band of the dehumidified plaster. Finally, the repair mortar A showed a great ductility behavior that can prevent the brittle delamination of the dehumidified plaster applied to damp masonry. For this reason, mortar A was selected to made the next mixed stone-mortar specimens and to analyze in this way the de-bonding problems for dehumidified plaster.

Table 1 Average mechanical and hygrometric values.

	$\sigma$ (N/mm <sup>2</sup> )	$E$ (N/mm <sup>2</sup> )	$W_{24}$ (daN/m <sup>3</sup> )
Mortar A	3.38	4,379	15.06
Mortar B	4.29	3,496	5.46

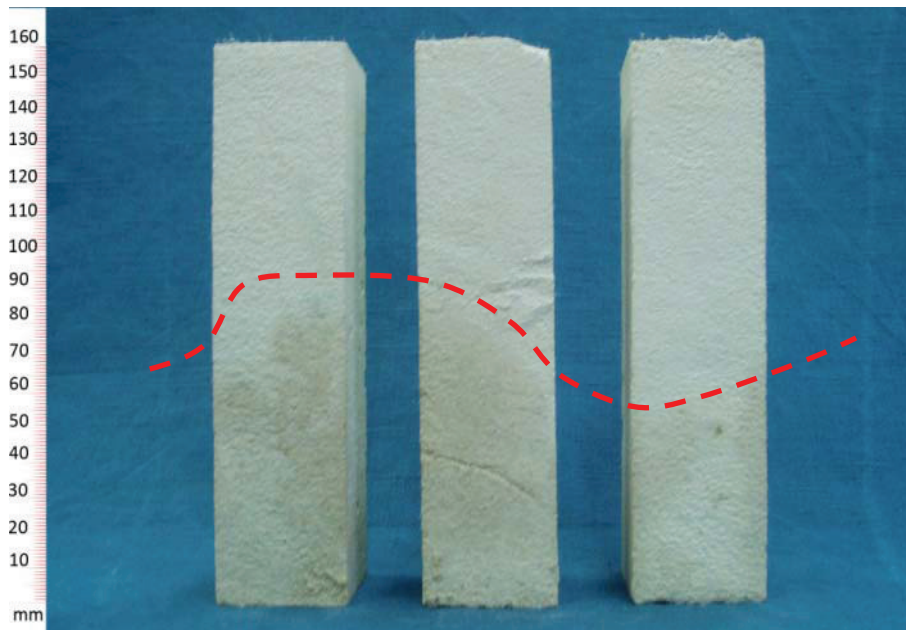


Fig. 11 Lift height of capillarity in specimens mortar B.

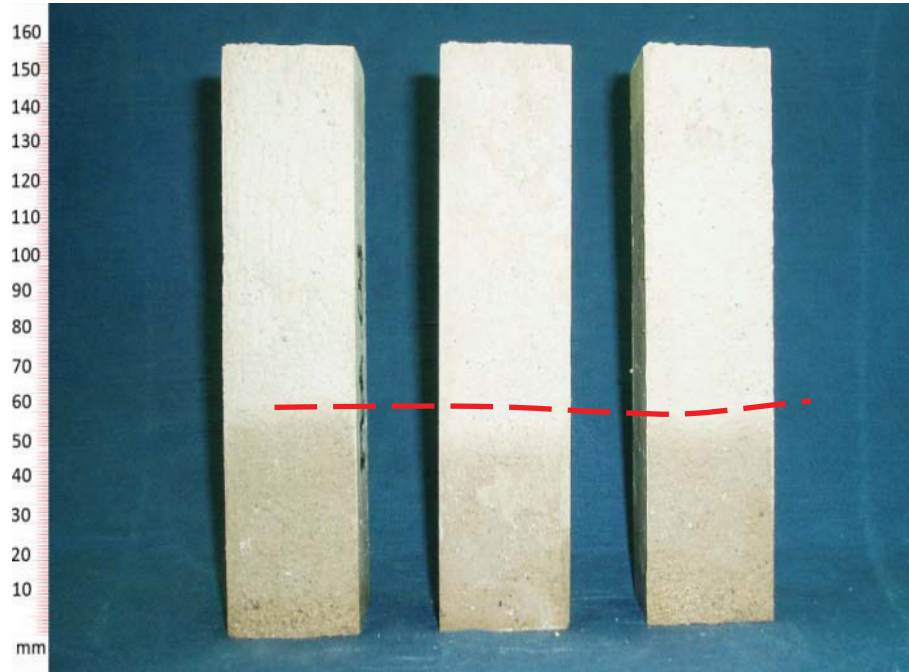


Fig. 12 Lift height of capillarity in specimens mortor A.

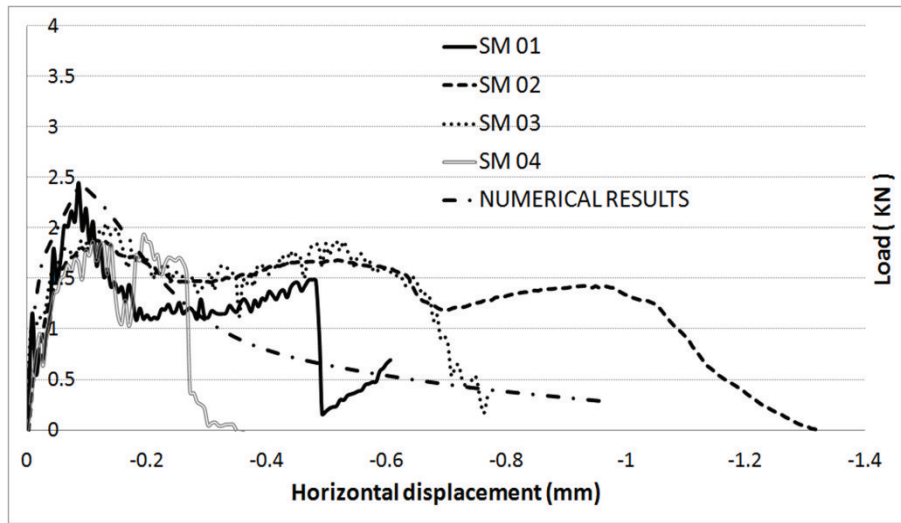


Fig. 13 Load-horizontal displacement curves of static tests.

3.2 Composite Stone-Repair Mortar Specimens

The results of compressive static tests are showed in Fig. 13 and in Table 2. The composite specimens stone-mortar were displayed four stress singularity points: two notch tips at the specimen top, and two at the specimen bottom (Fig. 13). These points were the weakest planes involved in the singular stress fields. Because of the wedges, the cracks that start from the bottom of the specimen have showed a greater

velocity than the cracks that start from the top of the specimen.

Table 2 Experimental results of static tests on mixed specimens stone-repair mortar.

Specimen	Max load (N)	Max horizontal displacement (mm)
SM 01	2,530	0.6077
SM 02	1,910	1.3218
SM 03	2,100	0.7695
SM 04	1,970	0.3629

To exception of SM 04, the other composite specimens were displayed a ductil behavior keeping a residual load and displacement after the peak load (Fig. 13). That is a fundamental requirement for a durable service life of repair plasters subjected to thermo-higrometric cycles stress as rising damp effects. The specific geometry of the composite specimens has allowed to test the adherence between dehumidified repair plaster and masonry structures, in order to pre-qualify the durability of the repair product. The notch tips have put to the test the adherence of the repair plaster applied to the stone support, simulating the fatigue loads that can compromise the restoration work.

The teflon sheet, inserted at the contact surface between the upper and lower wedge, was able to reduce the friction and to stabilize the load curves.

The static compressive tests represent a rather fast laboratory procedure useful for analyse the delamination of the dehumidified repair plasters applied to the historical masonry of the Sacri Monti di Varallo. The next step of this experimental research, at the moment in progress, is to carry out the cyclic compressive tests in order to simulate the fatigue stress between the masonry stone and the repair mortar.

#### 4. Numerical Analysis through the Cohesive Crack Model

The most realistic method used today for the numerical simulation of mortar and stone block fracture is the cohesive crack model, also known as Barenblatt-Dugdale-Hillerborg model for quasi-brittle materials. In the present work, the crack initiation criterion is assumed as:

$$\left(\frac{\sigma_0}{f_i}\right)^2 + \left(\frac{\tau_0}{f_s}\right)^2 = 1 \quad (1)$$

where,  $\sigma_0$  and  $\tau_0$  are stresses evaluated along the directions normal and tangential to the interface and  $f_i$  and  $f_s$  are the related strength. The point where Eq. (1) is satisfied is called fictitious crack tip.

According to this method, the cohesive stresses

acting on the non-linear FPZ (fracture process zone) are decreasing functions of the effective value of the displacement discontinuity [5-10]. In the present work, it was assumed:

$$w_{eff} = \sqrt{\left(\frac{w_n}{w_{nc}}\right)^2 + \left(\frac{w_t}{w_{tc}}\right)^2} \quad (2)$$

where,  $w_n$  is the mutual displacement component normal to the interface and  $w_t$  is the tangential one.  $w_{nc}$  and  $w_{tc}$  are the related critical values.

If  $w_{eff} > 1$ , no stress transfer occurs and the crack is therefore stress free, otherwise, the stresses are decreasing functions of  $w_{eff}$  that follow a pre-defined softening law. In the present work, the above mentioned law is assumed as follows [11]:

$$\frac{\sigma}{\sigma_0} = \frac{\tau}{\tau_0} = \left[1 - \frac{1 - \exp(-\alpha \cdot w_{eff})}{1 - \exp(-\alpha)}\right] \quad (3)$$

where, it is assumed  $\alpha = 5$ . The point where is  $w_{eff} = 1$  is called real crack tip. The behaviour of the material outside the FPZ is linear elastic.

In a symmetric model, it is well known [12-14] that the fracture process starts symmetrically, but loses this property before the peak load is reached. In order to simulate numerically this experimental evidence, a realistic scatter in strength was assumed, as shown in Table 3.

Therefore, the collapse is determined by a de-bonding process occurring on the right (weaker) side. Table 4 shows the elastic properties assumed.

The numerical analysis were executed through the ABAQUS code [15] by applying a pre-defined downward velocity to the upper face of the stone block. The deformed finite element mesh shown in Fig. 14.

**Table 3 Interface parameters.**

	$f_i$ (N/mm <sup>2</sup> )	$f_s$ (N/mm <sup>2</sup> )	$w_{nc}$ (mm)	$w_{tc}$ (mm)
Right side	0.2097	0.3159	0.5	0.5
Left side	0.2178	0.3249	0.5	0.5

**Table 4 Elastic properties.**

	Young's module (N/mm <sup>2</sup> )	Poisson ratio
Mortar	3,942	0.15
Stone	21,600	0.20



**Fig. 14** Finite element mesh at the maximum load, displacements are enlarged 100 times.

## 5. Experimental and Numerical Results

A preliminary elastic analysis shows four points of stress singularities: two notch tips on the specimen top, and two on the specimen bottom (Fig. 14). From these points, four cohesive cracks start to propagate along the bi-material interfaces, which are the weakest planes involved into the singular stress fields.

Because of the wedges (Fig. 14), the cracks starting from the specimen bottom show a growing velocity larger than the cracks starting from the specimen top. Therefore, the second couple of cracks plays the role of main cracks. The surface treatment shown in Fig. 8 increases the values of  $w_{nc}$  and  $w_{tc}$  in comparison to the case of the interface between the same type of mortar and brick [14].

Therefore, the loss of symmetry does not occur any longer at the peak load, but it occurs at the end of the softening phase and it causes the specimen collapse.

Fig. 11 show that the teflon sheet, inserted at the contact surface between upper and lower wedge, is able to reduce the friction and therefore it reduces the load values too. In the numerical simulation, the friction is disregarded. Numerical and experimental results are in good agreement (Fig. 13).

## 6. Conclusions

An innovative laboratory procedure for pre-qualification of dehumidified repair mortars applied to historical masonry buildings has been described. After a selection between two dehumidified mortars among the main repair market products, compression static tests are carried out on composite specimens stone block—repair mortar. Their specific geometry can test the de-bonding process of mortar in adherence with the historical masonry structures.

This method supplies useful indication to select, from a range of alternatives, the repair product that is best in keeping with the mechanical characteristics of historical material. In this way, it is possible avoid errors associated with materials that are not mechanically compatible.

The experimental procedure is currently being used at Sacro Monte di Varallo Special Natural Reserve (UNESCO heritage site) in Piedmont (Italy), where the historical stone masonry of the Chapels are subjected to rising damp effects due to capillary action or rain infiltrations. The study of the phenomena involved in the de-bonding process between the masonries stone and the dehumidified repair plasters is basic to plan a durable restoration work of the historical plasters of the Chapels in Sacri Monti di Varallo.

A numerical simulation based on the cohesive crack model was used to follow the experimental data. The evolutionary phenomena involved in the de-bonding process of mortar in a coupled stone block—mortar system are accurately analyzed by means of the experimental setup proposed. Through the cohesive crack model, it was possible to interpret theoretically the above mentioned phenomena occurring at the interface between stone block and mortar. Therefore, the mechanical behavior of the interface is characterized. The parameters obtained can be used for the analysis of a problem with different boundary conditions.

## Acknowledgments

The financial support provided by the Piedmont Region RE-FRESCOS Project is gratefully acknowledged.

## References

- [1] A. Grazzini, Experimental techniques for the evaluation of the durability of strengthening works on historical masonry, *Masonry International* 19 (2006) 113-126.
- [2] P. Bocca, A. Grazzini, Experimental procedure for the pre-qualification of strengthening mortars, *International Journal of Architectural Heritage* 6 (3) (2012) 302-321.
- [3] P. Bocca, A. Grazzini, Mechanical properties and freeze-thaw durability of strengthening mortars, *Journal of Materials in Civil Engineering* 25 (2) (2013) 274-280.
- [4] P. Bocca, A. Grazzini, Durability evaluation of strengthening mortars applied to historical masonry structures, in: *Proceedings of the Second International Conference on Sustainable Construction Materials and Technologies*, Italy, June 2010, pp. 1419-1429.
- [5] J. Cervenka, J.M.C. Kishen, V.E. Saouma, Mixed mode fracture of cementitious bimaterial interfaces—Part II: Numerical simulations, *Engineering Fracture Mechanics* 60 (1998) 95-107.
- [6] F. Barpi, S. Valente, Fuzzy parameters analysis of time-dependent fracture of concrete dam models, *International Journal of Numerical and Analytical Method in Geomechanics* 26 (2002) 1005-1027.
- [7] F. Barpi, S. Valente, A fractional order rate approach for modeling concrete structures subjected to creep and fracture, *International Journal of Solids and Structures* 41 (9-10) (2004) 2607-2621.
- [8] F. Barpi, S. Valente, Lifetime evaluation of concrete structures under sustained post-peak loading, *Engineering Fracture Mechanics* 72 (2005) 2427-2443.
- [9] F. Barpi, S. Valente, Modeling water penetration at dam-foundation joint, *Engineering Fracture Mechanics* 75 (3-4) (2008) 629-642.
- [10] F. Barpi, S. Valente, The cohesive frictional crack model applied to the analysis of the dam-foundation joint, *Engineering Fracture Mechanics* 77 (2010) 2182-2191.
- [11] H.A.W. Cornelissen, D.A. Hordijk, H.W. Reinhardt, Experimental determination of crack softening characteristics of normal and lightweight concrete, *Heron* 31 (1986) 45-56.
- [12] F. Barpi, S. Valente, Size-effects induced bifurcation phenomena during multiple cohesive crack propagation, *International Journal of Solids and Structures* 35 (16) (1998) 1851-1861.
- [13] A. Alberto, P. Antonaci, S. Valente, Damage analysis of brick-to-mortar interfaces, in: *Proceedings of 11th International Conference on the Mechanical Behavior of Materials*, Como Lake, Italy, 2011, pp. 1151-1156.
- [14] P. Bocca, A. Grazzini, D. Masera, A. Alberto, S. Valente, Mechanical interaction between historical brick and repair mortar: Experimental and numerical tests, *Journal of Physics* 305 (2011) 1-10.
- [15] ABAQUS 6.10 User's Manual, Dassault System Simulia Corp., Providence, RI, USA, 2010.